

THE IMPACT OF FORWARD SWEEP ON TIP CLEARANCE FLOWS IN TRANSONIC COMPRESSORS

Aspi R. Wadia*, Chunill Hah**, Douglas Rabe***

*GE Aircraft Engines, **NASA Glenn Research Center, ***Wright Labs, USAF

Keywords: *Transonic, Compressors, Forward-Sweep, Clearance Flows*

Abstract

The paper presents an analytical study of tip clearance flows in transonic compressor rotors using a 3D Navier Stokes solver. The numerical code, that was calibrated with test data from a single stage transonic compressor rig using an aft swept transonic compressor rotor at two radial clearance levels, was exercised to examine two different compressor rotor configurations, one with a conventional radial leading edge profile and the other with forward sweep. Evaluations were done at multiple rotor tip clearance levels to obtain clearance sensitivities with respect to flow, efficiency and stall margin. The forward swept rotor blades while demonstrating improvements in stall margin and efficiency showed significant reduction in clearance sensitivity. While the efficiency benefits with forward sweep were more pronounced at the nominal tip clearance, the large stall margin benefits were retained at all clearance levels studied. Detailed comparisons of the tip shock structure, span-wise re-distribution of the flow and the subsequent reduction in tip loading in terms of the static pressure rise are used to explain the flow mechanisms responsible for the reduction in tip sensitivity with forward sweep.

1 Introduction

Tip flow fields of high-speed, low-aspect ratio compressors are a large source of loss and blockage and dominate performance levels and, in many cases are highly sensitive to tip clearance levels, making them less desirable

from an operability stand point. How well the blades in a compressor tolerate open clearances due to several factors such as deterioration, casing ovalization and thermal mismatching of the rotor and stator structures determines how effectively it operates in service in the field. Correlations, such as those by Smith [1], to determine the losses due to tip clearance were developed based on low speed compressor tests.

Current transonic fan and compressor blade designs have been moving in the direction to use aerodynamic sweep to improve the performance and stability of compression components [2,3,4]. The experimental and analytical studies of single- and multi-stage transonic fans by Wadia et al.[2,5] demonstrated significant improvements in efficiency and stall margin attributed to forward sweep. The primary flow mechanisms responsible for the performance improvements with forward sweep were identified as reduced shock/boundary layer interaction and less accumulation of centrifuged blade suction side boundary layer fluid at the tip. This fundamental effect of forward sweep to alter the span-wise flow distribution by pulling more flow toward the tip of the blade results in reduction in tip loading. Low speed tests have shown that this reduced tip loading with forward sweep has a beneficial effect on the tip leakage blockage and this paper's CFD analysis will show this benefit is retained even in the presence of strong shocks.

Low speed tests to exploit sweep and desensitize compressor blades to the detrimental effects of tip clearance flows have been conducted by Yamaguchi [6], Inou [7] and

McNulty [8]. Yamaguchi showed a 1% improvement in compressor stage efficiency with forward sweep but with reduced stall margin. A weak hub in Yamaguchi's design may have been responsible for the reduced stall margin. Inou's low speed studies with forward sweep yielded a 0.7% improvement in stage peak efficiency along with about 7% improvement in stall margin. McNulty presented low speed results with similar conclusions as Inou and showed reduced clearance sensitivity with forward swept blades.

This paper presents the results of an analytical study of tip clearance flows in transonic compressor rotors using a 3D Navier Stokes solver. The tip clearance effect is limited only to the rotor; the impact on the overall stage performance is not considered herein. The rotor configurations came from a single stage transonic rig design [9] that models the front stages of advanced aircraft engine high-pressure ratio multistage fans. The code, developed at NASA by Hah [10,11] and used in this paper, has been calibrated with test data [12] using an aft swept transonic compressor rotor at two radial clearance levels. This code was exercised herein to examine the tip clearance flows in two different compressor rotor configurations, one with a conventional radial leading edge profile and the other with forward sweep. Evaluations were done at tip clearance levels of 0.02" (20 mils, nominal), 0.04" (40 mils, intermediate) and 0.08" (80 mils, large) corresponding to tip clearance to tip chord ratios of 0.5, 1.0 and 2 percent, respectively and tip clearance to average blade height ratios of 0.4, 0.8 and 1.6 percent.

The forward swept rotor blades while demonstrating improvements in stall margin and efficiency showed significant reduction in clearance sensitivity. While the efficiency benefits with forward sweep were more pronounced at the nominal tip clearance, the stall margin benefits were retained at all clearance levels studied. Detailed comparisons of the tip shock structure, span-wise redistribution of the flow and the subsequent reduction in tip loading in terms of the static pressure rise are used to explain the flow

mechanisms responsible for the reduction in tip sensitivity with forward sweep.

2 Rotor Design Summary

Table 1 summarizes the relevant design parameters that were held constant between the two rotor configurations used in the analytical evaluation. Both rotor configurations selected for this study came from the design of a single stage transonic rig [9] shown in Fig. 1.

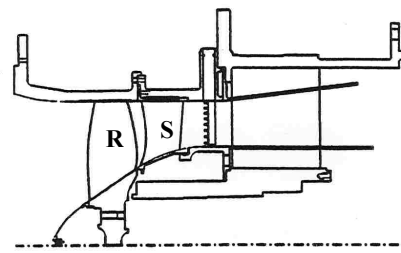


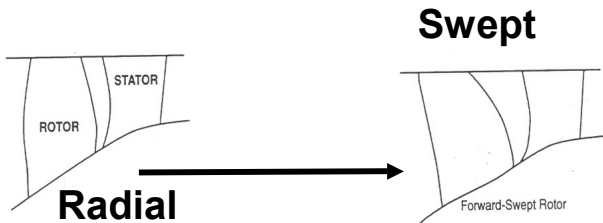
Fig. 1. Single-stage transonic compressor rig

Table 1 Rotor Key Design Parameters

<u>Parameters</u>	
Inlet Specific Flow	43.61 lbm/sec-ft ²
Inlet Corrected Tip Speed	1500 ft/sec
Inlet Corrected Flow	61.81 lb/sec
Stage Pressure Ratio	1.92
Rotor Design Pressure Ratio	2.06
Inlet Radius Ratio	0.312
Tip Diameter	17 in.
Number of Rotors/Stators	20/37
Aspect Ratio (Rotor/Stator)	1.32/1.26
Solidity (Rotor/Stator)	2.30/1.68
Tip Stagger Angle (Radial)	59.8 Deg.
Tip Stagger Angle (Swept)	55.5 Deg.

The radial and forward swept rotor detailed design and test results at the nominal clearance level have been reported by Wadia et al.[2]. The key effect of forward swept rotors is that it alters the radial flow distribution by pulling more flow up toward the blade tip. During the design process the forward swept rotor's mean camber lines were re-shaped in response to this flow shift by opening the blade sections near the tip and closing the remaining airfoil sections to maintain similar blade leading edge incidence

angles along the span and to match the radial rotor's exit total pressure profile. This is the reason for the reduced tip stagger angle of the forward swept rotor in Table 1. Fig. 2 shows schematics and pictures of the rotors.



[Comparison of Rotor Planforms](#)



[Radial Rotor Blisk](#)

[Swept Rotor Blisk](#)

Fig. 2. Schematic of radial and forward swept rotors and rotor blisk photos.

The reduction in tip loading with forward sweep is a result of the span wise flow shift in conjunction with radial equilibrium giving similar static pressure rise but with a higher dynamic head. As both rotor configurations were tested [2] to be tip limited, the reduced tip loading of the forward swept rotor results in more stable flow range. Subsequent 3D CFD analyses that follow later in the paper will show the beneficial effects that this reduced tip loading has on the tip-leakage flow.

3 Numerical Method

Although significant progress has been made in numerical techniques in the last few years, obtaining an accurate numerical solution of the flow field inside a transonic compressor rotor remains challenging. The development of three-dimensional boundary layers on the blade surface and end-walls, as well as shock-boundary layer interaction, and the tip clearance

flow, needs to be accurately calculated to capture the overall flow field correctly.

For the current study, the governing equations are solved with a pressure-based implicit relaxation method using a fully conservative control volume approach. A standard two-equation turbulence model is used, modified to include the low Reynolds number effects. A third-order accurate interpolation scheme is used for the discretization of the convection terms and central differencing is used for the diffusion terms. The method is of second-order accuracy with smoothly varying grids.

The computational grid was generated to give an orthogonal grid near the leading edge and near the blade surface where the most important flow phenomena (passage shock, shock-boundary layer interaction, etc.) occur. With this grid, spatial periodicity at the periodic surfaces is not enforced for the grid, so the physical periodicity condition is accounted for inside the code using an interpolation function. The grid consists of 61 nodes in the blade-to-blade direction, 56 nodes in the span wise direction, and 162 nodes in the stream wise direction. Ten computational nodes are actually distributed on the blade tip to describe the blade tip geometry and ten nodes are located between the blade tip and the shroud. As a very small change in the size of the tip clearance changes the flow structure significantly, especially in transonic blades, the precise hot geometry of the blade tip was correctly modeled in the current study. The standard boundary conditions for the transonic flow in a compressor are used and the residuals of each finite difference equation are integrated over the entire domain. When the integrated residuals of all the equations are reduced by four orders of magnitude from their initial value, the solution is considered to have converged. Each operating condition requires about three Cray YMP single-processor CPU hours to get a fully converged solution.

The numerical scheme described above has been applied by Copenhaver et al.[12] to experimental data from an aft swept rotor tested in the same single stage transonic compressor rig at two clearance levels. Other than being

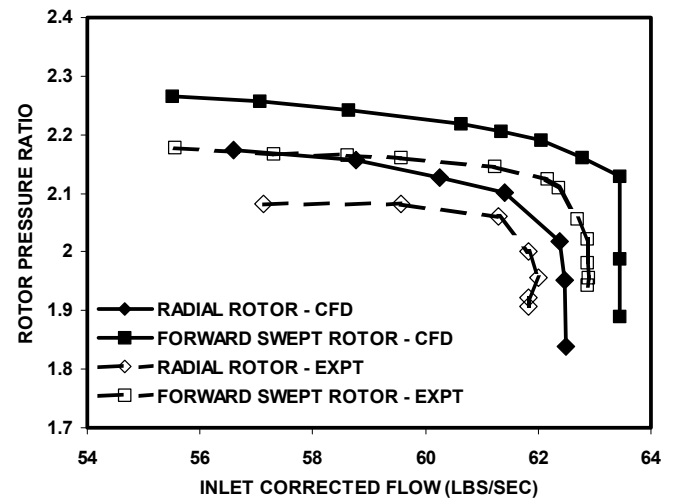
swept aft, this rotor is similar in design to the two rotors being evaluated in this article. While the absolute value of the rotor efficiency calculated by this code was slightly lower relative to data, the decrease in rotor performance due to the increase in tip clearance was in very good agreement with the test data. The numerical solution predicted slightly higher pressure rise than the measured value at both clearance levels.

The numerical scheme described above is also validated herein using experimental data [2] for the radial and forward swept rotor tested in the single stage transonic compressor rig. Although the experiment was performed with a rotor/stator combination, the test results presented here are for only the rotor. The overall rotor performance was determined from stator leading edge instrumentation distributed on four different stator vanes. Radial traverse data between the rotor and the stator, available at one circumferential position up to 80% immersion, was only used to compare the shape of the radial profiles with the analyses later in the paper.

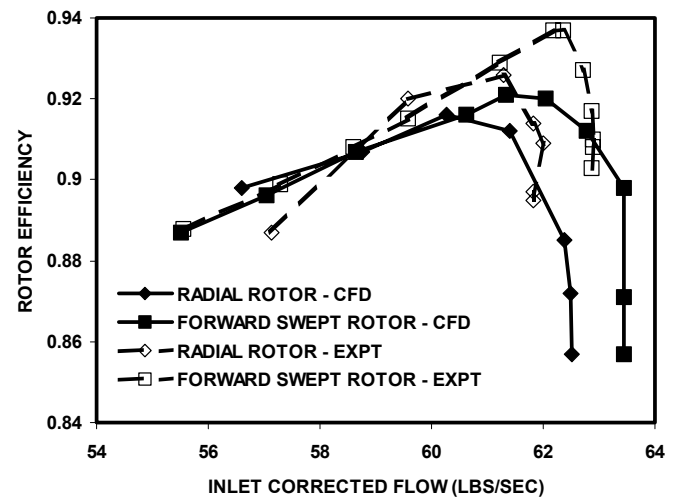
Fig. 3 shows the comparison of the measured and calculated rotor performance for both rotors at design speed tested with nominal clearance. The calculated results are generally in good agreement with the test data.

As shown in Fig. 3a, the forward swept rotor flows more than the radial rotor and this difference in flow is accurately calculated by the numerical method. The absolute value of the calculated design flow is approximately 1% higher than the test data for both rotors. In the rig test, the forward swept rotor demonstrated approximately 6% more stall margin than the radial rotor. The calculated stall points shown in the figure represent the lowest inlet corrected flow beyond which the numerical solution became unstable. The relative difference in stall margin between the two rotors is predicted very well by the numerical analysis.

While the calculated rotor efficiencies (Fig. 3b) are between 0.7 to 1.5% lower than the data, the difference in peak efficiency between the forward swept and radial rotor obtained from the numerical analysis is in good agreement.



(a)



(b)

Fig. 3. Comparison of measured and calculated rotor (alone) performance: (a) pressure ratio, (b) adiabatic efficiency; for the radial and forward swept rotors.

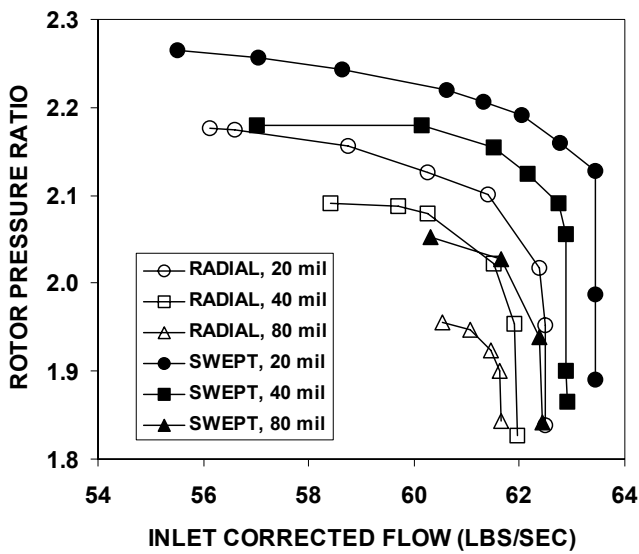
3 Results and Discussion

The primary objective of the present study is to do a parametric study on the effect of tip clearance size on fan performance with radial and forward swept rotors.

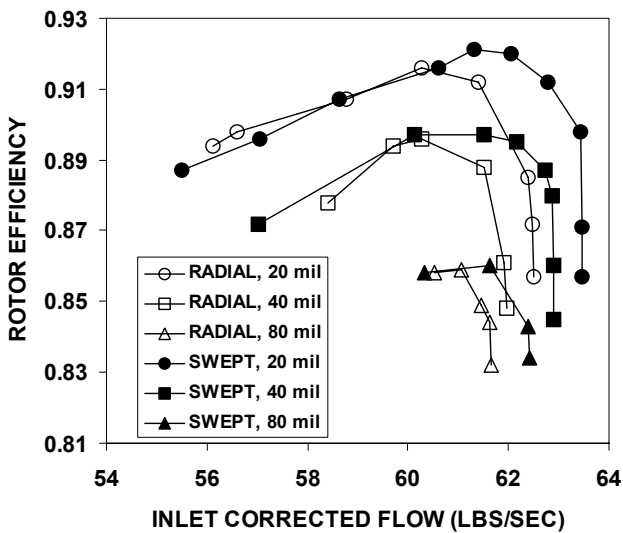
3.1 Overall Rotor Performance

The calculated performance at the three clearance levels at design speed is presented in Fig. 4. The lowest flow points in the figure

represent the last stable point predicted before the numerical code failed to converge.



(a)



(b)

Fig. 4. Comparison of calculated rotor performance: (a) rotor pressure ratio, (b) rotor adiabatic efficiency.

The performance map in Fig. 4a shows the forward swept rotor to pump more with more pressure rise than the radial rotor along a nominal operating line. The forward swept rotor shows 6.8% higher throttle margin than the radial rotor with more flow range and peak pressure rise at the nominal clearance condition. The fact that the swept rotor stalls at the same

flow but at a much larger pressure ratio than the radial rotor at the most open tip clearance condition attests to the beneficial influence forward sweep has on tip leakage flow.

The efficiency characteristics at the nominal clearance condition in Fig. 4b show that the forward swept rotor achieved a peak efficiency that is 0.5% higher than the radial rotor. However, at the intermediate and large clearance levels the forward swept rotor achieved a peak efficiency that is only 0.1% higher than the radial rotor. Thus for this forward swept rotor configuration, the numerical calculations suggest significant advantage of forward sweep on stable operating range and efficiency at nominal clearance levels and significant stable operating range but with only small efficiency benefit at large clearance levels.

3.2 Tip Clearance Sensitivity

The standard compressor performance data are presented in a slightly different format in Fig. 5 to better quantify the differences in clearance sensitivity. This allows the clearance derivatives to be compared between the swept and radial blades. The change in stall margin with clearance is plotted versus the ratio of clearance to tip chord, the change in peak efficiency is plotted versus the ratio of tip clearance to average blade height and the loss in flow (choked) divided by the choked flow with the nominal clearance is plotted versus change in tip clearance from the nominal clearance condition.

The sensitivity of peak efficiency to clearance is shown in Fig. 5a. While the forward swept rotor showed higher peak efficiency than the radial rotor at all clearance levels analyzed, the swept rotor's clearance derivative is about 20% higher at the intermediate clearance level and about the same as that of the radial rotor at larger clearances.

Fig. 5b presents the sensitivity of the stall margin, a measure of stable operating range, to rotor tip clearance. As seen in the rotor performance map in Fig. 4a, forward sweep has

at least 5.5% more stall margin than the radial rotor at all clearance levels investigated. In this case the radial rotor's clearance derivative is about 15% higher at the mid- clearance level and once again about the same as that of the forward swept rotor at larger clearances. The

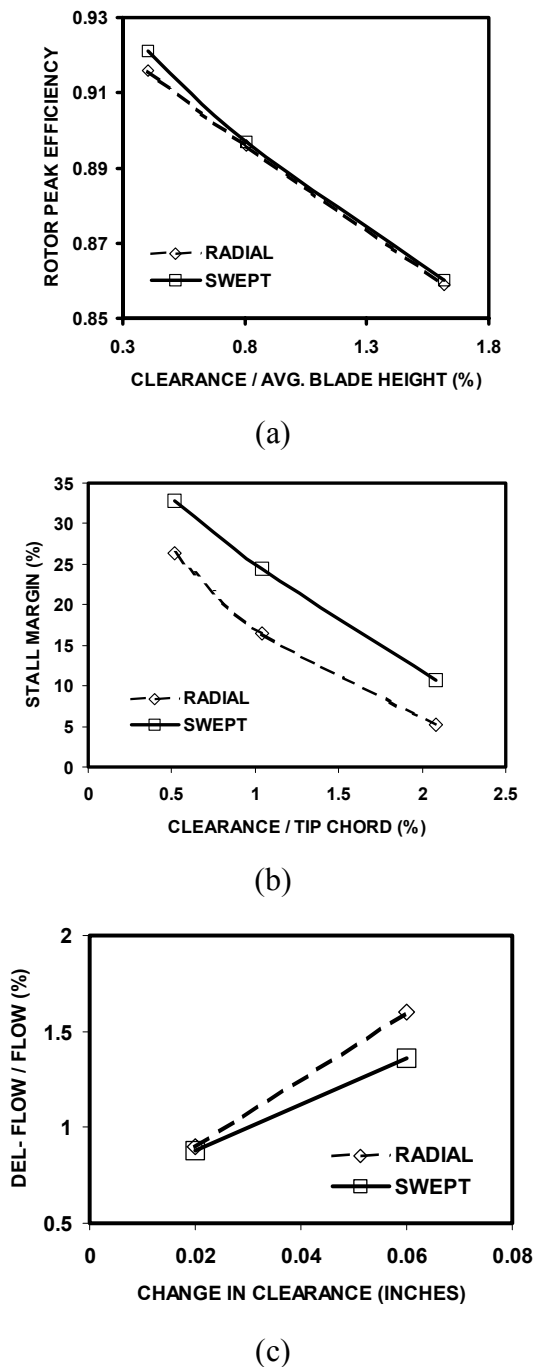


Fig. 5. Calculated rotor tip-clearance sensitivity: (a) peak efficiency, (b) stall margin, (c) Change in choked flow.

results suggest that forward sweep improves the blade's tip loading capability at a given clearance and significantly reduces its sensitivity to open clearances.

The flow sensitivity to tip clearance is presented in Fig. 5c. While the forward swept rotor flows more than the radial rotor at all conditions, the reduction in flow due the first 0.02 inches change in clearance is about the same for both rotors. However, at the large clearance condition the radial rotor incurs significantly more flow loss than the swept rotor. The pumping capability of the swept rotor even at large clearances is significantly better than that of the radial rotor, an especially good attribute in multi-stage applications. It should be noted that the presence of a downstream stator, not accounted for in this analysis, could affect the overall pumping capability in the rig test.

3.3 Radial Profiles

The comparison of the radial distribution of rotor airfoil section efficiencies calculated from the total pressure and total temperature profiles measured using a radial traverse probe at one circumferential position between the rotor and the stator at peak efficiency for the nominal clearance case is presented in Fig. 6. The profiles indicate that most of the tip loss in efficiency occurs in the outermost 10 to 15% of the blade. The radial rotor tip efficiency is about 7% lower than that for the swept blade. The forward swept blade also shows some improvement in efficiency in the mid-span region.

Fig. 7 shows the comparison of the rotor efficiencies between the radial and swept rotors at peak efficiency with nominal and large clearances from the CFD results. At the nominal clearance, the radial rotor's performance at the casing is about 4% less than that of the swept rotor. This localized difference in performance between the two rotors is about half that in the test data shown Fig. 6 and can be attributed to steady flow and turbulence modeling assumptions in the analysis. Below 50% immersion the swept rotor performance is

generally better than that of the radial rotor similar to the data in Fig. 6.

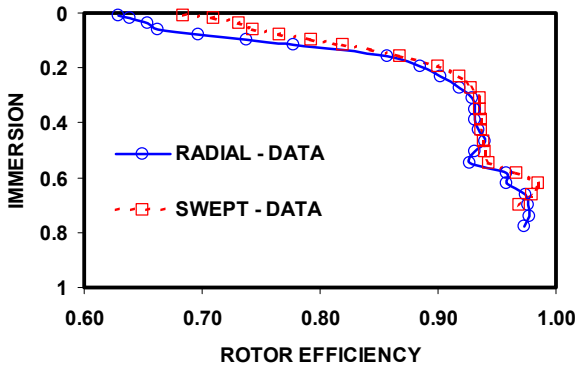


Fig. 6. Measured radial efficiency profile comparisons at peak efficiency with nominal clearance.

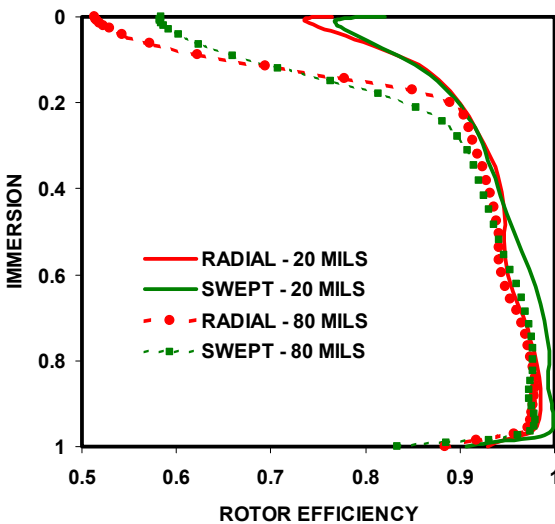


Fig. 7. Calculated efficiency radial profile comparisons at peak efficiency with nominal and large clearances.

In the case with the large clearance, a different response in the span wise sense is indicated between the swept and radial rotors. The swept rotor shows about 9% higher efficiency at the casing than the radial blade. However, the radial blade’s efficiency is better than that of the swept rotor from about 13% immersion to slightly below the blade mid span region.

At the nominal and large clearance levels the radial profiles show that the forward swept rotor incurs a loss in efficiency across the entire span with the larger clearance, while most of the

penalty in performance for the radial rotor is limited to the top 25% of the blade. The swept blade maybe significantly less sensitive to the larger tip clearance in the vicinity of the blade tip, but the rest of the blade suffers which ultimately results in almost no improvement in it’s overall rotor performance relative to the radial rotor as shown in Fig. 4b.

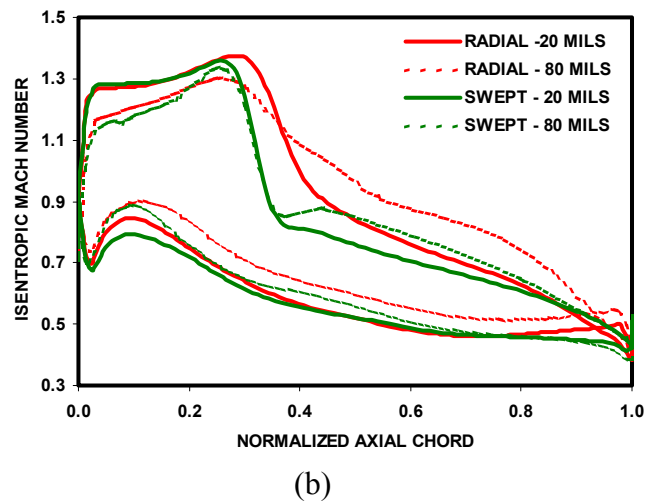
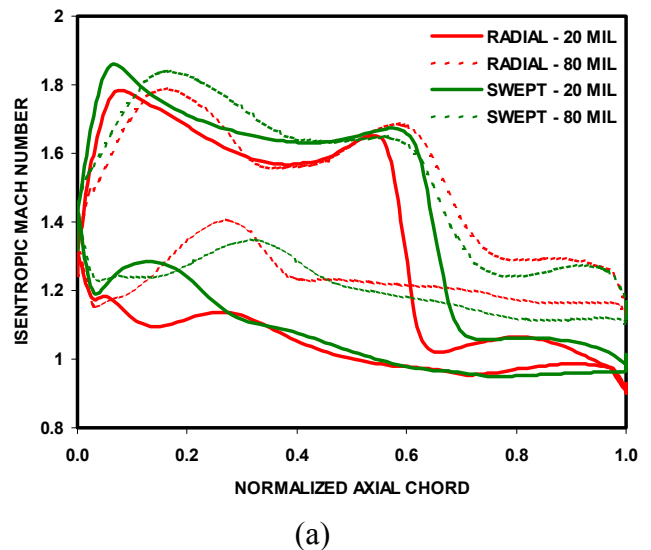


Fig. 8. Comparison of blade surface isentropic Mach number distributions at peak efficiency: (a) blade tip and (b) mid-span.

The blade surface isentropic Mach number distributions at peak efficiency for both rotors at the nominal and large clearance levels are presented in Fig. 8 at two span wise locations. The calculated blade-to-blade tip static pressure

contours for both rotors at nominal clearance at peak efficiency and near stall are shown in Fig.9.

At the blade tip (Figs. 8a and 9a), at nominal clearance, the radial rotor has a single shock system with the suction surface shock located at 55% from the leading edge. At the same clearance level, the forward swept rotor has a two-shock system (Figs. 8a and 9c) with the suction surface shock located further downstream at 60% and a weak pressure surface shock at 12% axial distance from the leading edge, respectively. Both blades have about the same level of loading (lift) downstream of the shock. This two-shock system with forward sweep at the peak efficiency point on the map (Fig. 4b) may be responsible for limiting the overall efficiency difference between the two rotors in the blade-tip region as shown in Fig. 7.

At nominal clearance, Fig. 8b shows that the location of the suction surface shock at mid span is reversed between the two rotors; the radial blade now having a more over-expanded shock structure than the swept blade resulting in lower efficiencies for the radial rotor in the bottom half of the blade relative to the swept blade as shown in Fig. 7.

The reduction in the airfoil lift distribution at the blade tip with the large clearance relative to the nominal clearance condition for both rotors is evident in Fig. 8a. The reduction in lift is more for the radial blade and it's stronger over-expansion shock contributes to the penalty in performance at the blade tip as illustrated in Fig. 7. At mid-span the radial rotor adjusts to a shock-free configuration at the large clearance and shows a negligible penalty in performance between the nominal and large clearance conditions. The swept rotor, which now has a stronger over expanded shock structure, indicates a significant performance penalty with the larger clearance across its entire inner span.

As the rotors are throttled to stall, Fig. 9 shows the bow shock strengthens and migrates upstream detaching from the leading edge. The forward swept rotor with its strengthened tip has capability to throttle further resulting in higher stall margin as shown in Fig.4a.

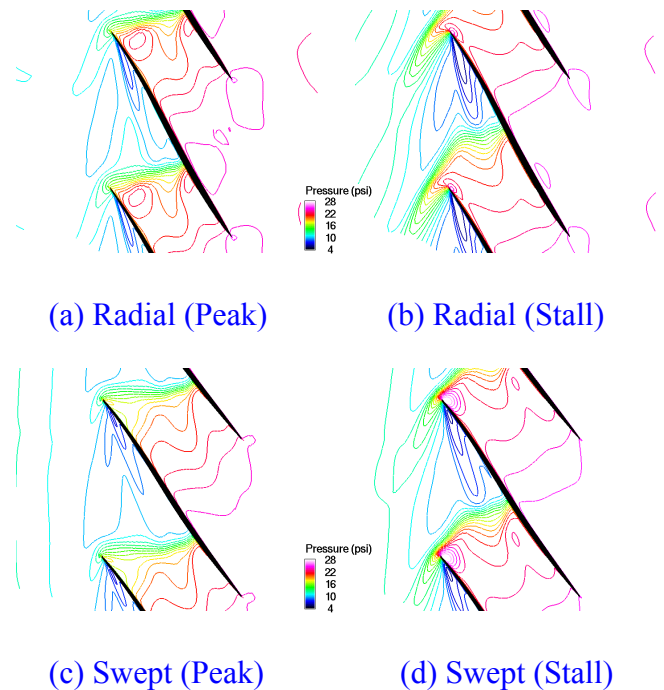


Fig. 9 Comparison of blade-to-blade static pressure contours at peak efficiency and near stall with nominal clearance.

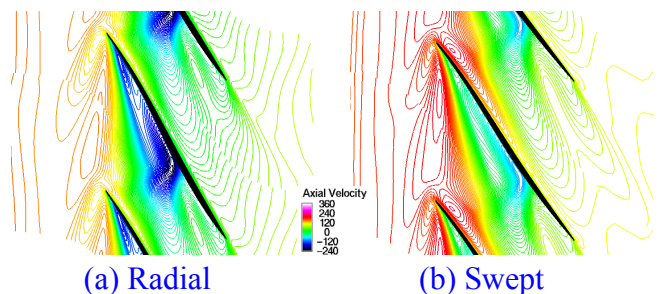


Fig. 10. Comparison of blade-to-blade axial velocity contours at mid clearance at peak efficiency with nominal clearance.

The blade-to-blade axial velocity contours in the gap with nominal clearance at peak efficiency are presented in Fig. 10. The regions of reverse flow (negative axial velocity) are shown in dark blue and light blue colors.

Common to both rotors, much of the leakage flow exits from the clearance gap into the passage with a negative axial velocity component. The negative velocities are the highest where the tip leakage flow intersects with the shock near the suction surface of the airfoil. The reverse flow is detrimental to the

rotor’s aerodynamic stability as it resists the scrubbed casing boundary layer fluid.

Significant differences in the tip leakage flow are also apparent in Fig. 10. The forward swept blade has a much smaller reverse flow region with very little penetration into the blade passage. The increased flow into the tip, a characteristic with forward sweep, increases the stream wise momentum of the swept rotor’s leakage flow, consequently reducing the negative axial component. Downstream of the vortex leading edge, the swept rotor’s leakage flow has slightly higher velocities and its tip blockage is concentrated further aft in the passage and farther away from the adjacent blade’s pressure surface.

Fig. 11 compares cross-stream axial velocity contours at rotor trailing edge for both rotors near stall with nominal and large clearances. Recall, that the forward swept rotor has a higher total pressure ratio and more flow roll back at stall than the radial rotor as shown in Fig. 3. The low velocity fluid near the casing extending across the blade passage from the blade pressure to the suction side is attributed to tip leakage flow. The figure clearly shows the tip leakage flow to be a large source of blockage (and loss) even at the nominal clearance condition. This source of blockage increases significantly with the large clearance as shown in the figure. Based on the comparisons of the radial profile of efficiency between the analysis and data shown in Figs. 7 and 8, the actual penetration of blockage and subsequent increase in loss due to tip leakage flow is expected to be more severe in the experiment.

Qualitative comparison of velocity contours including at peak efficiency (not shown) suggest that the forward swept rotor has lower tip leakage blockage and outside the tip vortex the swept rotor has higher velocities in the outer panel. Near the hub the swept rotor has a slightly weaker suction surface boundary layer based on the density of the contours in that region.

Fig. 12 shows the cross-stream entropy contours at the trailing edge of both rotors near stall. The high loss fluid near the casing extending across the passage is also associated

with tip leakage flow. The forward swept rotor is seen to have lower loss near the pressure surface at the casing end-wall. However, in the suction surface corner the swept blade shows higher loss. This difference is a contribution to the noted difference in the surface Mach number distributions at mid span at the large clearance level.

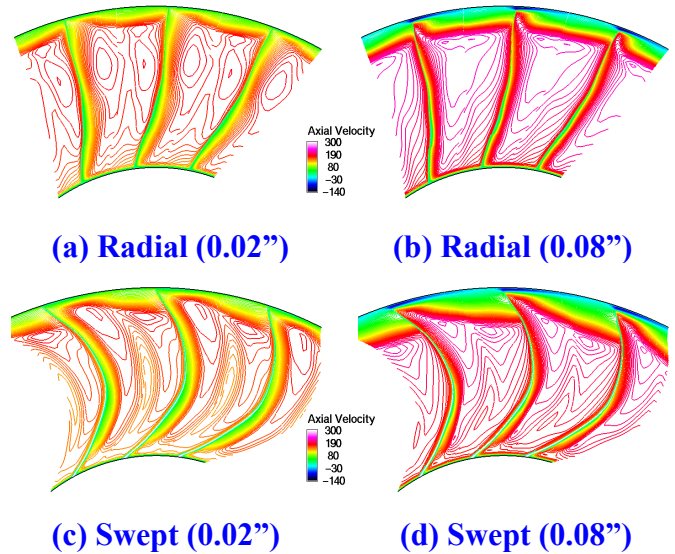


Fig. 11. Calculated cross-stream contours of axial velocity at rotor trailing edge near stall with nominal and large clearances.

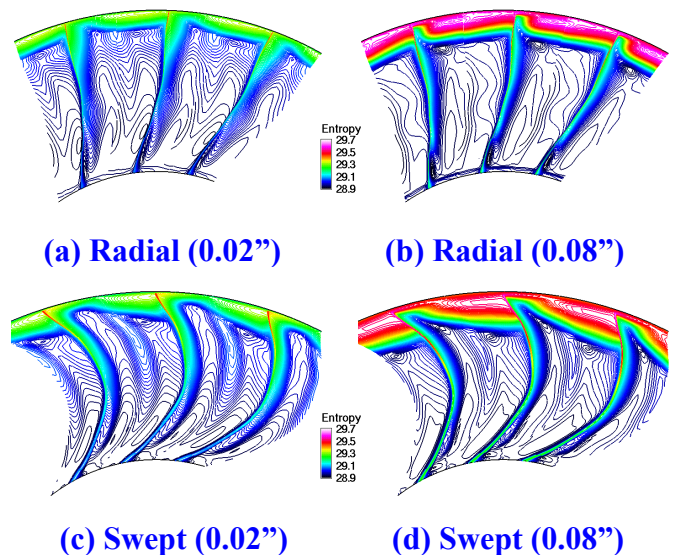


Fig. 12. Calculated cross-stream contours of entropy at rotor trailing edge near stall with nominal and large clearances.

4 Concluding Remarks

The results of a detailed analytical evaluation of the impact of forward sweep on tip clearance flows in transonic compressor rotors are presented. Evaluations were done for a radial and a forward swept rotor at peak efficiency and near stall at multiple clearances.

The forward swept rotor demonstrated improvements in efficiency and stall margin at all clearance levels analyzed. The difference in efficiency between the forward swept rotor and the radial rotor decreased with increasing levels of tip clearance. However, forward sweep demonstrated significant improvement in stall margin at all levels of clearance relative to the radial rotor. The improved loading capability with forward sweep is attributed to the radial shift in flow toward the tip and the subsequent reduction in tip loading levels. Numerical analyses showed forward sweep to provide a shallower tip vortex trajectory, reduced tip leakage blockage and smaller reversed flow region in the clearance gap.

From the discussion above it is apparent, that for transonic blades, not only is the tip clearance flow structure impacted by a change in gap height but the shock structure and the subsequent shock boundary layer interaction is affected across the entire blade span. Hence, the adjustment of blade camber levels to account for the detrimental effects of large gaps becomes crucial during the blade design.

5 Acknowledgements

The authors would like to acknowledge the support of Dr. Steven Puterbaugh and his team at the CARL facility (USAF) in obtaining the test data used in this paper.

References

- [1] Smith L. H. Casing boundary layers in multistage axial flow compressors. *Proceedings, Flow Research on Blading*. L.S. Dzung ed., Elsevier Publishing, Amsterdam, Netherlands, 1970.
- [2] Wadia A. R, Szucs P.N and Crall D.W. Inner workings of aerodynamic sweep. *Transactions of the ASME, Journal of Turbomachinery*, Vol. 120, No. 4, pp 671-682, October 1998.
- [3] Denton J. D and Xu I. The effects of lean and sweep on transonic fan performance. ASME Paper GT-2002-30327, Amsterdam, June 2002.
- [4] Gallimore S. J, Bolger J. J, Cumpsty N. A, Taylor M. J, Wright, P. I and Place J. M. The use of sweep and dihedral in multistage axial flow compressor blading Part II: Low and high speed designs and test verification. ASME Paper GT-2002-30329, Amsterdam, June 2002.
- [5] Wadia A. R, Szucs, P. N, Crall D. W and Rabe D. C. Forward swept rotor studies in multistage fans with inlet distortion. ASME Paper GT-2002-30326, Amsterdam, June 2002.
- [6] Yamaguchi N, Tominaga T, Hattori S and Mitsuhashi T. Secondary-loss reduction by forward skewing of axial compressor rotor blading. Presented at the 1991 Yokohama International Gas Turbine Conference, Yokohama, 1991.
- [7] Inou M, Kuroumaru M and Furukawa M. Controlled-endwall-flow blading for multistage axial compressor rotor. ASME paper 97-GT-248, Orlando, Florida, June 1997.
- [8] McNulty G, Decker J, Beacher B and Khalid S. A. The impact of forward swept rotors on tip limited low speed axial compressors, ASME paper GT-2003-38837, Atlanta, Georgia, June 2003.
- [9] Law C. H and Wadia A. R. Low aspect ratio transonic rotors Part I: Baseline design and performance. *Transactions of the ASME, Journal of Turbomachinery*, Vol. 115, No. 2, pp 218-225, April 1993.
- [10] Hah C. A numerical modeling of endwall and tip clearance flow of an isolated compressor rotor. *Transactions of the ASME. Journal of Engineering for Gas Turbines and Power*, Vol. 108, No. 1, pp 15-21, January 1986.
- [11] Hah, C. Calculation of three-dimensional viscous flows in turbomachines with an implicit relaxation method. *AIAA Journal of Propulsion and Power*, Vol. 3, No. 5, pp415-422, 1987.
- [12] Copenhaver, W, Mayhew E, Hah C and Wadia A. The effect of tip clearance on a swept transonic compressor rotor. *Transactions of the ASME, Journal of Turbomachinery*, Vol. 118, No. 2, pp 230-239, April 1996.